# ELEMENT MATERIALS TECHNOLOGY

(formerly PCTEST)
7185 Oakland Mills Road, Columbia, MD 21046 USA
Tel. +1.410.290.6652 / Fax +1.410.290.6654
http://www.element.com


# PART 0 SAR CHAR REPORT

**Applicant Name:**
Microsoft Corporation
One Microsoft Way
Redmond, WA 98052 USA

**Date of Testing:**
03/17/22 - 06/28/22
**Test Site/Location:**
Element, Columbia, MD, USA
**Document Serial No.:**
1M2204040049-01.C3K (Rev1)

## FCC ID: C3K1997

## APPLICANT: MICROSOFT CORPORATION

**Report Type:** Part 0 SAR Characterization
**DUT Type:** Portable Computing Device
**Model(s):** 1997

Note: This revised Test Report (S/N: 1M2204040049-01.C3K (Rev1)) supersedes and replaces the previously issued test report on the same subject device for the same type of testing as indicated. Please discard or destroy the previously issued test report(s) and dispose of it accordingly.

I attest to the accuracy of data. All measurements reported herein were performed by me or were made under my supervision and are correct to the best of my knowledge and belief. I assume full responsibility for the completeness of these measurements and vouch for the qualifications of all persons taking them.

Test results reported herein relate only to the item(s) tested.

RJ Ortanez
Executive Vice President

ACCREDITED
CERT #2041.01

# TABLE OF CONTENTS

# 1 DEVICE UNDER TEST

## 1.1 Device Overview

This device uses the Qualcomm® Smart Transmit feature to control and manage transmitting power in real time and to ensure the time-averaged RF exposure is in compliance with the FCC requirement at all times for 3G/4G/5G WWAN operations. Additionally, this device supports WLAN/BT technologies, but the output power of these modems is not controlled by the Smart Transmit algorithm.

| Band & Mode | Operating Modes | Tx Frequency |
|---|---|---|
| UMTS 850 | Data | 826.40 - 846.60 MHz |
| UMTS 1900 | Data | 1852.4 - 1907.6 MHz |
| LTE Band 71 | Data | 665.5 - 695.5 MHz |
| LTE Band 12 | Data | 699.7 - 715.3 MHz |
| LTE Band 13 | Data | 779.5 - 784.5 MHz |
| LTE Band 14 | Data | 790.5 - 795.5 MHz |
| LTE Band 26 (Cell) | Data | 814.7 - 848.3 MHz |
| LTE Band 5 (Cell) | Data | 824.7 - 848.3 MHz |
| LTE Band 66 (AWS) | Data | 1710.7 - 1779.3 MHz |
| LTE Band 4 (AWS) | Data | 1710.7 - 1754.3 MHz |
| LTE Band 25 (PCS) | Data | 1850.7 - 1914.3 MHz |
| LTE Band 2 (PCS) | Data | 1850.7 - 1909.3 MHz |
| LTE Band 30 | Data | 2307.5 - 2312.5 MHz |
| LTE Band 7 | Data | 2502.5 - 2567.5 MHz |
| LTE Band 41 | Data | 2498.5 - 2687.5 MHz |
| LTE Band 48 | Data | 3552.5 - 3697.5 MHz |
| NR Band n71 | Data | 665.5 - 695.5 MHz |
| NR Band n5 (Cell) | Data | 826.5 - 846.5 MHz |
| NR Band n66 (AWS) | Data | 1712.5 - 1777.5 MHz |
| NR Band n25 (PCS) | Data | 1852.5 - 1912.5 MHz |
| NR Band n2 (PCS) | Data | 1852.5 - 1907.5 MHz |
| NR Band n41 | Data | 2506.02 - 2679.99 MHz |
| NR Band n77 | Data | 3710.01 - 3969.99 MHz |
| 2.4 GHz WLAN | Data | 2412 - 2472 MHz |
| U-NII-1 | Data | 5180 - 5240 MHz |
| U-NII-2A | Data | 5260 - 5320 MHz |
| U-NII-2C | Data | 5500 - 5720 MHz |
| U-NII-3 | Data | 5745 - 5825 MHz |
| U-NII-5 | Data | 5935 - 6415 MHz |
| U-NII-6 | Data | 6435 - 6525 MHz |
| U-NII-7 | Data | 6535 - 6875 MHz |
| U-NII-8 | Data | 6895 - 7115 MHz |
| Bluetooth | Data | 2402 - 2480 MHz |
| NR Band n260 | Data | 37000 - 40000 MHz |
| NR Band n261 | Data | 27500 - 28350 MHz |

## 1.2 Time-Averaging for SAR and Power Density

This device is enabled with Qualcomm® Smart Transmit algorithm to control and manage transmitting power in real time and to ensure that the time-averaged RF exposure from 3G/4G/5G Sub-6 NR WWAN is in compliance with FCC requirements. This Part 0 report shows SAR characterization of WWAN radios for 3G/4G/5G Sub-6 NR. Characterization is achieved by determining $P_{Limit}$ for 3G/4G/5G Sub-6 NR that corresponds to the exposure design targets after accounting for all device design related uncertainties, i.e., SAR_design_target (< FCC SAR limit) for sub-6 radio. The SAR characterization is denoted as SAR Char in this report. Section 1.3 includes a nomenclature of the specific terms used in this report.

The compliance test under the static transmission scenario and simultaneous transmission analysis are reported in Part 1 report. The validation of the time-averaging algorithm and compliance under the dynamic (time- varying) transmission scenario for WWAN technologies are reported in Part 2 report (report SN could be found in Section 1.4 – Bibliography).

## 1.3 Nomenclature for Part 0 Report

| Technology | Term | Description |
|---|---|---|
| 3G/4G/5G Sub-6 NR | $P_{limit}$ | Power level that corresponds to the exposure design target (*SAR_design_target)* after accounting for all device design related uncertainties |
| | $P_{max}$ | Maximum tune up output power |
| | *SAR_design_target* | Target SAR level < FCC SAR limit after accounting for all device design related uncertainties |
| | *SAR Char* | Table containing *Plimit* for all technologies and bands |

## 1.4 Bibliography

| Report Type | Report Serial Number |
|---|---|
| Near Field PD Report (Part 1) | 1M2204040049-25.C3K |
| Near Field PD Part 0 Report | |
| RF Exposure Part 2 Test Report | 1M2204040049-21.C3K |
| RF Exposure Compliance Summary Report | 1M2204040049-27.C3K |
| RF Exposure Part 1 Test Report | 1M2204040049-02.C3K |

# 2 SAR AND POWER DENSITY MEASUREMENTS

## 2.1 SAR Definition

Specific Absorption Rate is defined as the time derivative (rate) of the incremental energy (dU) absorbed by (dissipated in) an incremental mass (dm) contained in a volume element (dV) of a given density (ρ). It is also defined as the rate of RF energy absorption per unit mass at a point in an absorbing body (see Equation 2-1).

**Equation 2-1**
**SAR Mathematical Equation**

$$SAR = \frac{d}{dt}\left(\frac{dU}{dm}\right) = \frac{d}{dt}\left(\frac{dU}{\rho dv}\right)$$

**SAR is expressed in units of Watts per Kilogram (W/kg).**

$$SAR = \frac{\sigma \cdot E^2}{\rho}$$

where:

| | | |
|---|---|---|
| σ | = | conductivity of the tissue-simulating material (S/m) |
| ρ | = | mass density of the tissue-simulating material (kg/m$^3$) |
| E | = | Total RMS electric field strength (V/m) |

NOTE: The primary factors that control rate of energy absorption were found to be the wavelength of the incident field in relation to the dimensions and geometry of the irradiated organism, the orientation of the organism in relation to the polarity of field vectors, the presence of reflecting surfaces, and whether conductive contact is made by the organism with a ground plane.[6]

## 2.2 SAR Measurement Procedure

The evaluation was performed using the following procedure compliant to FCC KDB Publication 865664 D01v01r04 and IEEE 1528-2013:

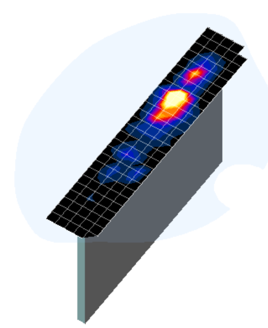

**Figure 2-1**
**Sample SAR Area Scan**

1. The SAR distribution at the exposed side of the head or body was measured at a distance no greater than 5.0 mm from the inner surface of the shell. The area covered the entire dimension of the device-head and body interface and the horizontal grid resolution was determined per FCC KDB Publication 865664 D01v01r04 (See Table 2-1) and IEEE 1528-2013.
2. The point SAR measurement was taken at the maximum SAR region determined from Step 1 to enable the monitoring of SAR fluctuations/drifts during the 1g/10g cube evaluation. SAR at this fixed point was measured and used as a reference value.
3. Based on the area scan data, the peak of the region with maximum SAR was determined by spline interpolation. Around this point, a volume was assessed according to the measurement resolution and volume size requirements of FCC KDB Publication 865664 D01v01r04 (See Table 2-1) and IEEE 1528-2013. On the

basis of this data set, the spatial peak SAR value was evaluated with the following procedure (see references or the DASY manual online for more details):

a. SAR values at the inner surface of the phantom are extrapolated from the measured values along the line away from the surface with spacing no greater than that in Table 2-1. The extrapolation was based on a least-squares algorithm. A polynomial of the fourth order was calculated through the points in the z-axis (normal to the phantom shell).

b. After the maximum interpolated values were calculated between the points in the cube, the SAR was averaged over the spatial volume (1g or 10g) using a 3D-Spline interpolation algorithm. The 3D-spline is composed of three one-dimensional splines with the “Not a knot” condition (in x, y, and z directions). The volume was then integrated with the trapezoidal algorithm. One thousand points (10 x 10 x 10) were obtained through interpolation, in order to calculate the averaged SAR.

c. All neighboring volumes were evaluated until no neighboring volume with a higher average value was found.

4. The SAR reference value, at the same location as step 2, was re-measured after the zoom scan was complete to calculate the SAR drift. If the drift deviated by more than 5%, the SAR test and drift measurements were repeated.

**Table 2-1**
**Area and Zoom Scan Resolutions per FCC KDB Publication 865664 D01v01r04***

| Frequency | Maximum Area Scan Resolution (mm) ($\Delta x_{area}$, $\Delta y_{area}$) | Maximum Zoom Scan Resolution (mm) ($\Delta x_{zoom}$, $\Delta y_{zoom}$) | Maximum Zoom Scan Spatial Resolution (mm) | | | Minimum Zoom Scan Volume (mm) (x,y,z) |
|---|---|---|---|---|---|---|
| | | | Uniform Grid | Graded Grid | | |
| | | | $\Delta z_{zoom}(n)$ | $\Delta z_{zoom}(1)$* | $\Delta z_{zoom}(n>1)$* | |
| ≤ 2 GHz | ≤ 15 | ≤ 8 | ≤ 5 | ≤ 4 | ≤ 1.5*$\Delta z_{zoom}(n-1)$ | ≥ 30 |
| 2-3 GHz | ≤ 12 | ≤ 5 | ≤ 5 | ≤ 4 | ≤ 1.5*$\Delta z_{zoom}(n-1)$ | ≥ 30 |
| 3-4 GHz | ≤ 12 | ≤ 5 | ≤ 4 | ≤ 3 | ≤ 1.5*$\Delta z_{zoom}(n-1)$ | ≥ 28 |
| 4-5 GHz | ≤ 10 | ≤ 4 | ≤ 3 | ≤ 2.5 | ≤ 1.5*$\Delta z_{zoom}(n-1)$ | ≥ 25 |
| 5-6 GHz | ≤ 10 | ≤ 4 | ≤ 2 | ≤ 2 | ≤ 1.5*$\Delta z_{zoom}(n-1)$ | ≥ 22 |

*Also compliant to IEEE 1528-2013 Table 6

# 3 SAR CHARACTERIZATION

## 3.1 DSI and SAR Determination

This device uses different Device State Index (DSI) to configure different time averaged power levels based on certain exposure scenarios. Depending on the detection scheme implemented in the smartphone, the worst-case SAR was determined by measurements for the relevant exposure conditions for that DSI. Detailed descriptions of the detection mechanisms are included in the operational description.

When 1g SAR and 10g SAR exposure comparison is needed, the worst-case was determined from SAR normalized to 1g or 10g SAR limit.

The device state index (DSI) conditions used in Table 3-1 represent different exposure scenarios.

**Table 3-1**
**DSI and Corresponding Exposure Scenarios**

| Scenario | Description | SAR Test Cases |
|---|---|---|
| Laptop mode (DSI = 3) | ▪ Device transmits in laptop mode when keyboard accessory is attached and at an angle ≤210° or no motion is detected | *Laptop SAR per KDB Publication 616217 D04v01r02* |
| Tablet Mode (DSI=6) | ▪ Device transmits in tablet when no keyboard accessory is attached, motion is detected, or keyboard accessory is attached at >210° angle | *Tablet SAR per KDB Publication 648474 D04v01r03* |

## 3.2 SAR Design Target

*SAR_design_target* is determined by ensuring that it is less than FCC SAR limit after accounting for total device designed related uncertainties specified by the manufacturer (see Table 3-2).

**Table 3-2**
***SAR_design_target* Calculations – Low Bands**

| ***SAR_design_target*** | |
|---|---|
| $SAR\_design\_target < SAR\_regulatory\_limit \times 10^{\frac{-Total\ Uncertainty}{10}}$ | |
| **1g SAR (W/kg)** | |
| *Total Uncertainty* | 1.0 dB |
| *SAR_regulatory_limit* | 1.6 W/kg |
| *SAR_design_target* | 0.8 W/kg |

Note: Low Bands refer to UMTS B5, LTE B71/12/13/14/26/5, NR Bands n71/5

**Table 3-3**
***SAR_design_target* Calculations – Mid/High Bands**

| ***SAR_design_target*** | |
|---|---|
| $SAR\_design\_target < SAR\_regulatory\_limit \times 10^{\frac{-Total\ Uncertainty}{10}}$ | |
| **1g SAR (W/kg)** | |
| *Total Uncertainty* | 1.0 dB |
| *SAR_regulatory_limit* | 1.6 W/kg |
| *SAR_design_target* | 1.0 W/kg |

Note: Mid Bands refer to UMTS B2, LTE B66/4/25/2, NR Bands n66/n25/n2; High Bands refer to LTE B30/7/41 PC3/41 PC2/48, NR Bands n41/77

## 3.3 SAR Char

SAR test results corresponding to *Pmax* for each antenna/technology/band/DSI can be found in Appendix A.

*Plimit* is calculated by linearly scaling with the measured SAR at the Ppart0 to correspond to the *SAR_design_target*. When *Plimit* < *Pmax*, *Ppart0* was used as Plimit in the Smart Transmit EFS. When *Plimit* > *Pmax* and *Ppart0*=Pmax, calculated *Plimit* was used in the Smart Transmit EFS. All reported SAR obtained from the Ppart0 SAR tests was less than *SAR_Design_target*+ 1 dB Uncertainty. The final *Plimit* determination for each exposure scenario corresponding to *SAR_design_target* are shown in Table 3-3.

**Table 3-4**
***PLimit* Determination**

| Device State Index (DSI) | *PLimit* Determination Scenarios |
|---|---|
| 3 | $P_{limit}$ is calculated based on 1g Body Laptop SAR at 0 mm for bottom edge with keyboard accessory attached. |
| 6 | $P_{limit}$ is calculated based on 1g Body Tablet SAR at 0 mm for back, top, bottom, right, and left surfaces with and without keyboard accessory. |

## Table 3-5
## SAR Characterizations

| Exposure Senario | | Laptop Mode | Tablet Mode | Maximum Tune-Up Output Power* |
|---|---|---|---|---|
| Averaging Volume | | 1g | 1g | |
| Spacing | | 0 mm | 0 mm | |
| Configuration | | Laptop | Tablet | |
| DSI | | 3 | 6 | |
| Technology/Band | Antenna | | | Pmax |
| UMTS 850 | 4 | 30.0 | 16.7 | 24.4 |
| UMTS 1900 | 1 | 30.0 | 12.6 | 24.4 |
| LTE Band 71 | 4 | 30.0 | 14.7 | 24.0 |
| LTE Band 12 | 4 | 30.0 | 16.3 | 24.3 |
| LTE Band 13 | 4 | 30.0 | 16.4 | 24.0 |
| LTE Band 14 | 4 | 30.0 | 16.5 | 24.0 |
| LTE Band 26 (Cell) | 4 | 30.0 | 16.7 | 24.5 |
| LTE Band 5 (Cell) | 4 | 30.0 | 16.7 | 24.5 |
| LTE Band 66/4 (AWS) | 1 | 30.0 | 13.9 | 24.5 |
| LTE Band 25/2 (PCS) | 1 | 30.0 | 12.6 | 24.4 |
| LTE Band 30 | 1 | 30.0 | 11.8 | 23.0 |
| LTE Band 7 | 1 | 30.0 | 11.3 | 24.0 |
| LTE Band 48 | 2 | 30.0 | 9.0 | 22.0 |
| LTE Band 41 (PC3) | 1 | 30.0 | 11.3 | 22.0 |
| LTE Band 41 (PC2) | 1 | 30.0 | 11.3 | 22.9 |
| NR Band n71 | 4 | 30.0 | 14.7 | 24.0 |
| NR Band n5 (Cell) | 4 | 30.0 | 16.7 | 24.2 |
| NR Band n66 (AWS) | 1 | 30.0 | 14.7 | 24.5 |
| NR Band n66 (AWS) | 4 | 30.0 | 14.2 | 24.5 |
| NR Band n25/n2 (PCS) | 1 | 30.0 | 12.6 | 24.2 |
| NR Band n25/n2 (PCS) | 4 | 30.0 | 13.5 | 24.2 |
| NR Band n41 | 1 | 30.0 | 11.3 | 24.0 |
| NR Band n41 | 4 | 30.0 | 13.5 | 24.0 |
| NR Band n41 | 5 | 30.0 | 10.0 | 22.0 |
| NR Band n41 | 8 | 30.0 | 10.0 | 22.0 |
| NR Band n77 | 2 | 30.0 | 7.4 | 24.5 |
| NR Band n77 | 3 | 30.0 | 7.0 | 24.5 |
| NR Band n77 | 5 | 30.0 | 8.0 | 22.5 |
| NR Band n77 | 8 | 30.0 | 8.0 | 22.5 |

**Notes:**

1. When $P_{max} < P_{limit}$, the DUT will operate at a power level up to $P_{max}$.

# 4 EQUIPMENT LIST

## For SAR measurements

| Manufacturer | Model | Description | Cal Date | Cal Interval | Cal Due | Serial Number |
|---|---|---|---|---|---|---|
| Agilent | E4404B | Spectrum Analyzer | N/A | N/A | N/A | MY45113242 |
| Agilent | E4438C | ESG Vector Signal Generator | 5/10/2022 | Annual | 5/10/2023 | MY42082659 |
| Agilent | E4438C | ESG Vector Signal Generator | 3/24/2022 | Annual | 3/24/2023 | MY45093678 |
| Agilent | N5182A | MXG Vector Signal Generator | 6/21/2021 | Annual | 6/21/2022 | MY47420603 |
| Agilent | N5182A | MXG Vector Signal Generator | 1/12/2022 | Annual | 1/12/2023 | MY47420837 |
| Agilent | 8753ES | S-Parameter Vector Network Analyzer | 2/11/2022 | Annual | 2/11/2023 | MY40003841 |
| Agilent | 8753ES | S-Parameter Vector Network Analyzer | 4/14/2021 | Annual | 4/14/2022 | US39170118 |
| Agilent | E5515C | Wireless Communications Test Set | 5/12/2022 | Annual | 5/12/2023 | GB43304278 |
| Agilent | E5515C | Wireless Communications Test Set | 5/4/2021 | Biennial | 5/4/2023 | GB41450275 |
| Agilent | N4010A | Wireless Connectivity Test Set | N/A | N/A | N/A | GB46170464 |
| Amplifier Research | 15S1G6 | Amplifier | CBT | N/A | CBT | 433974 |
| Amplifier Research | 15S1G6 | Amplifier | CBT | N/A | CBT | 343972 |
| Anritsu | ML2496A | Power Meter | 4/21/2021 | Annual | 4/21/2022 | 1351001 |
| Anritsu | ML2496A | Power Meter | 3/29/2022 | Annual | 3/29/2023 | 1306009 |
| Anritsu | MA2411B | Pulse Power Sensor | 4/29/2022 | Annual | 4/29/2023 | 1207470 |
| Anritsu | MA2411B | Pulse Power Sensor | 3/28/2022 | Annual | 3/28/2023 | 1339007 |
| Anritsu | MT8821C | Radio Communication Analyzer MT8821C | 3/31/2022 | Annual | 3/31/2023 | 6201664756 |
| Anritsu | MT8821C | Radio Communication Analyzer MT8821C | 5/11/2022 | Annual | 5/11/2023 | 6262044715 |
| Anritsu | MT8821C | Radio Communication Analyzer MT8821C | 9/26/2021 | Annual | 9/26/2022 | 6201524637 |
| Anritsu | MT8821C | Radio Communication Analyzer MT8821C | 8/10/2021 | Annual | 8/10/2022 | 6262150000 |
| Anritsu | MT8000A | Radio Communication Test Station | 8/2/2021 | Annual | 8/2/2022 | 6272337438 |
| Anritsu | MT8000A | Radio Communication Test Station | 4/15/2022 | Annual | 4/15/2023 | 6272337439 |
| Anritsu | MT8000A | Radio Communication Test Station | 8/2/2021 | Annual | 8/2/2022 | 6272337436 |
| Anritsu | MA24106A | USB Power Sensor | 4/22/2022 | Annual | 4/22/2023 | 1344556 |
| Anritsu | MA24106A | USB Power Sensor | 3/28/2022 | Annual | 3/28/2023 | 1520503 |
| Control Company | 4353 | Long Stem Thermometer | 10/28/2020 | Biennial | 10/28/2022 | 200670623 |
| Control Company | 4353 | Long Stem Thermometer | 10/28/2020 | Biennial | 10/28/2022 | 200670633 |
| Control Company | 4353 | Long Stem Thermometer | 10/28/2020 | Biennial | 10/28/2022 | 200670635 |
| Control Company | 4040 | Therm./ Clock/ Humidity Monitor | 1/21/2022 | Annual | 1/21/2023 | 160574418 |
| Control Company | 4040 | Therm./ Clock/ Humidity Monitor | 3/12/2021 | Biennial | 3/12/2023 | 210202100 |
| Mitutoyo | 500-196-30 | CD-6"ASX 6Inch Digital Caliper | 2/16/2022 | Triennial | 2/16/2025 | A20238413 |
| Keysight Technologies | N6705B | DC Power Analyzer | 5/5/2021 | Triennial | 5/5/2024 | MY53004059 |
| Keysight Technologies | N9020A | MXA Signal Analyzer | 4/14/2022 | Annual | 4/14/2023 | MY48010233 |
| MCL | BW-N6W5+ | 6dB Attenuator | CBT | N/A | CBT | 1139 |
| Mini-Circuits | VLF-6000+ | Low Pass Filter DC to 6000 MHz | CBT | N/A | CBT | N/A |
| Mini-Circuits | VLF-6000+ | Low Pass Filter DC to 6000 MHz | 7/6/2021 | Annual | 7/6/2022 | 31634 |
| Mini-Circuits | BW-N20W5+ | DC to 18 GHz Precision Fixed 20 dB Attenuator | CBT | N/A | CBT | N/A |
| Mini-Circuits | NLP-1200+ | Low Pass Filter DC to 1000 MHz | CBT | N/A | CBT | N/A |
| Mini-Circuits | NLP-2950+ | Low Pass Filter DC to 2700 MHz | CBT | N/A | CBT | N/A |
| Mini-Circuits | BW-N20W5 | Power Attenuator | CBT | N/A | CBT | 1226 |
| Mini-Circuits | ZUDC10-83-S+ | Directional Coupler | CBT | N/A | CBT | 2050 |
| Narda | 4772-3 | Attenuator (3dB) | CBT | N/A | CBT | 9406 |
| Narda | BW-S3W2 | Attenuator (3dB) | CBT | N/A | CBT | 120 |
| Seekonk | TSF-100 | Torque Wrench | 7/8/2021 | Annual | 7/8/2022 | 47639-29 |
| Rohde & Schwarz | CMW500 | Wideband Radio Communication Tester | 4/18/2022 | Annual | 4/18/2023 | 128633 |
| Rohde & Schwarz | CMW500 | Wideband Radio Communication Tester | 1/11/2022 | Annual | 1/11/2023 | 101699 |
| Rohde & Schwarz | CMW500 | Wideband Radio Communication Tester | 4/8/2022 | Annual | 4/8/2023 | 162125 |
| Rohde & Schwarz | CMW500 | Wideband Radio Communication Tester | 4/7/2022 | Annual | 4/7/2023 | 167283 |
| SPEAG | DAK-3.5 | Dielectric Assessment Kit | 1/6/2022 | Annual | 1/6/2023 | 1278 |
| SPEAG | DAKS-3.5 | Portable Dielectric Assessment Kit | 8/18/2021 | Annual | 8/18/2022 | 1041 |
| SPEAG | DAKS-3.5 | Portable Dielectric Assessment Kit | 10/7/2021 | Annual | 10/7/2022 | 1045 |
| SPEAG | MAIA | Modulation and Audio Interference Analyzer | N/A | N/A | N/A | 1379 |
| SPEAG | MAIA | Modulation and Audio Interference Analyzer | N/A | N/A | N/A | 1237 |
| SPEAG | D750V3 | 750 MHz SAR Dipole | 3/14/2022 | Annual | 3/14/2023 | 1054 |
| SPEAG | D750V3 | 750 MHz SAR Dipole | 6/20/2019 | Triennial | 6/20/2022 | 1057 |
| SPEAG | D750V3 | 750 MHz SAR Dipole | 9/8/2021 | Annual | 9/8/2022 | 1097 |
| SPEAG | D835V2 | 835 MHz SAR Dipole | 1/21/2021 | Biennial | 1/21/2023 | 4d132 |
| SPEAG | D835V2 | 835 MHz SAR Dipole | 6/20/2019 | Triennial | 6/20/2022 | 4d040 |
| SPEAG | D835V2 | 835 MHz SAR Dipole | 10/19/2021 | Annual | 10/19/2022 | 4d133 |
| SPEAG | D850V2 | 850 MHz SAR Dipole | 9/8/2020 | Biennial | 9/8/2022 | 1010 |
| SPEAG | D850V2 | 850 MHz SAR Dipole | 12/7/2021 | Annual | 12/7/2022 | 1009 |
| SPEAG | D1750V2 | 1750 MHz SAR Dipole | 9/9/2020 | Biennial | 9/9/2022 | 1104 |
| SPEAG | D1765V2 | 1750 MHz SAR Dipole | 5/14/2021 | Biennial | 5/14/2023 | 1008 |
| SPEAG | D1900V2 | 1900 MHz SAR Dipole | 8/10/2020 | Biennial | 8/10/2022 | 5d180 |
| SPEAG | D1900V2 | 1900 MHz SAR Dipole | 9/10/2020 | Biennial | 9/10/2022 | 5d181 |
| SPEAG | D2600V2 | 2300 MHz SAR Dipole | 11/10/2020 | Biennial | 11/10/2022 | 1064 |
| SPEAG | D2450V2 | 2450 MHz SAR Dipole | 8/18/2021 | Annual | 8/18/2022 | 719 |
| SPEAG | D2450V2 | 2450 MHz SAR Dipole | 9/20/2020 | Biennial | 9/20/2022 | 797 |
| SPEAG | D2600V2 | 2600 MHz SAR Dipole | 6/14/2019 | Triennial | 6/14/2022 | 1064 |
| SPEAG | D3500V2 | 3500 MHz SAR Dipole | 1/21/2020 | Triennial | 1/21/2023 | 1097 |
| SPEAG | D3700V2 | 3700 MHz SAR Dipole | 1/19/2021 | Biennial | 1/19/2023 | 1018 |
| SPEAG | D3900V2 | 3900 MHz SAR Dipole | 6/10/2021 | Annual | 6/10/2022 | 1073 |
| SPEAG | D5GHzV2 | 5 GHz SAR Dipole | 1/10/2022 | Annual | 1/10/2023 | 1057 |
| SPEAG | D5GHzV2 | 5 GHz SAR Dipole | 9/15/2021 | Annual | 9/15/2022 | 1191 |
| SPEAG | DAE4 | Dasy Data Acquisition Electronics | 8/4/2021 | Annual | 8/4/2022 | 1680 |
| SPEAG | DAE4 | Dasy Data Acquisition Electronics | 5/11/2021 | Annual | 5/11/2021 | 701 |
| SPEAG | DAE4 | Dasy Data Acquisition Electronics | 1/13/2022 | Annual | 1/13/2023 | 793 |
| SPEAG | DAE4 | Dasy Data Acquisition Electronics | 11/11/2021 | Annual | 11/11/2022 | 1646 |
| SPEAG | DAE4 | Dasy Data Acquisition Electronics | 12/8/2021 | Annual | 12/8/2022 | 859 |
| SPEAG | DAE4 | Dasy Data Acquisition Electronics | 8/6/2021 | Annual | 8/6/2022 | 1683 |
| SPEAG | DAE4 | Dasy Data Acquisition Electronics | 4/13/2022 | Annual | 4/13/2023 | 501 |
| SPEAG | DAE4 | Dasy Data Acquisition Electronics | 8/3/2021 | Annual | 8/3/2022 | 1681 |
| SPEAG | DAE4 | Dasy Data Acquisition Electronics | 4/14/2022 | Annual | 4/14/2023 | 1402 |
| SPEAG | DAE4 | Dasy Data Acquisition Electronics | 3/22/2022 | Annual | 3/22/2023 | 604 |
| SPEAG | DAE4 | Dasy Data Acquisition Electronics | 2/22/2022 | Annual | 2/22/2023 | 1403 |
| SPEAG | DAE4 | Dasy Data Acquisition Electronics | 6/21/2021 | Annual | 6/21/2022 | 1676 |
| SPEAG | DAE4 | Dasy Data Acquisition Electronics | 8/16/2021 | Annual | 8/16/2022 | 1450 |
| SPEAG | DAE4 | Dasy Data Acquisition Electronics | 2/22/2022 | Annual | 2/22/2023 | 665 |
| SPEAG | DAE4 | Dasy Data Acquisition Electronics | 2/24/2022 | Annual | 2/24/2023 | 467 |
| SPEAG | EX3DV4 | SAR Probe | 9/20/2021 | Annual | 9/20/2022 | 7552 |
| SPEAG | EX3DV4 | SAR Probe | 5/18/2021 | Annual | 5/18/2022 | 7416 |
| SPEAG | EX3DV4 | SAR Probe | 1/19/2022 | Annual | 1/19/2023 | 3837 |
| SPEAG | EX3DV4 | SAR Probe | 11/16/2021 | Annual | 11/16/2022 | 7639 |
| SPEAG | EX3DV4 | SAR Probe | 1/10/2022 | Annual | 1/10/2023 | 7571 |
| SPEAG | EX3DV4 | SAR Probe | 9/6/2021 | Annual | 9/6/2022 | 7674 |
| SPEAG | EX3DV4 | SAR Probe | 4/22/2022 | Annual | 4/22/2023 | 7532 |
| SPEAG | EX3DV4 | SAR Probe | 8/5/2021 | Annual | 8/5/2022 | 7670 |
| SPEAG | EX3DV4 | SAR Probe | 2/21/2022 | Annual | 2/21/2023 | 7308 |
| SPEAG | EX3DV4 | SAR Probe | 4/22/2022 | Annual | 4/22/2023 | 7546 |
| SPEAG | EX3DV4 | SAR Probe | 3/22/2022 | Annual | 3/22/2023 | 7421 |
| SPEAG | EX3DV4 | SAR Probe | 2/22/2022 | Annual | 2/22/2023 | 7427 |
| SPEAG | EX3DV4 | SAR Probe | 7/20/2021 | Annual | 7/20/2022 | 7406 |
| SPEAG | EX3DV4 | SAR Probe | 6/28/2021 | Annual | 6/28/2022 | 7661 |
| SPEAG | EX3DV4 | SAR Probe | 2/22/2022 | Annual | 2/22/2023 | 7417 |

Note:

1. CBT (Calibrated Before Testing). Prior to testing, the measurement paths containing a cable, amplifier, attenuator, coupler or filter were connected to a calibrated source (i.e. a signal generator) to determine the losses of the measurement path. The power meter offset was then adjusted to compensate for the measurement system losses. This level offset is stored within the power meter before measurements are made. This calibration verification procedure applies to the system verification and output power measurements. The calibrated reading is then taken directly from the power meter after compensation of the losses for all final power measurements.
2. Each equipment item was used solely within its respective calibration period.

## 5 MEASUREMENT UNCERTAINTIES

### For SAR Measurements

| a | b | c | d | e= f(d,k) | f | g | h = c x f/e | i = c x g/e | k |
|---|---|---|---|---|---|---|---|---|---|
| Uncertainty Component | IEEE 1528 Sec. | Tol. (± %) | Prob. Dist. | Div. | $c_i$ 1gm | $c_i$ 10 gms | 1gm $u_i$ (± %) | 10gms $u_i$ (± %) | $v_i$ |
| Measurement System | | | | | | | | | |
| Probe Calibration | E.2.1 | 7 | N | 1 | 1 | 1 | 7.0 | 7.0 | ∞ |
| Axial Isotropy | E.2.2 | 0.25 | N | 1 | 0.7 | 0.7 | 0.2 | 0.2 | ∞ |
| Hemishperical Isotropy | E.2.2 | 1.3 | N | 1 | 0.7 | 0.7 | 0.9 | 0.9 | ∞ |
| Boundary Effect | E.2.3 | 2 | R | 1.732 | 1 | 1 | 1.2 | 1.2 | ∞ |
| Linearity | E.2.4 | 0.3 | N | 1 | 1 | 1 | 0.3 | 0.3 | ∞ |
| System Detection Limits | E.2.4 | 0.25 | R | 1.732 | 1 | 1 | 0.1 | 0.1 | ∞ |
| Modulation Response | E.2.5 | 4.8 | R | 1.732 | 1 | 1 | 2.8 | 2.8 | ∞ |
| Readout Electronics | E.2.6 | 0.3 | N | 1 | 1 | 1 | 0.3 | 0.3 | ∞ |
| Response Time | E.2.7 | 0.8 | R | 1.732 | 1 | 1 | 0.5 | 0.5 | ∞ |
| Integration Time | E.2.8 | 2.6 | R | 1.732 | 1 | 1 | 1.5 | 1.5 | ∞ |
| RF Ambient Conditions - Noise | E.6.1 | 3 | R | 1.732 | 1 | 1 | 1.7 | 1.7 | ∞ |
| RF Ambient Conditions - Reflections | E.6.1 | 3 | R | 1.732 | 1 | 1 | 1.7 | 1.7 | ∞ |
| Probe Positioner Mechanical Tolerance | E.6.2 | 0.8 | R | 1.732 | 1 | 1 | 0.5 | 0.5 | ∞ |
| Probe Positioning w/ respect to Phantom | E.6.3 | 6.7 | R | 1.732 | 1 | 1 | 3.9 | 3.9 | ∞ |
| Extrapolation, Interpolation & Integration algorithms for Max. SAR Evaluation | E.5 | 4 | R | 1.732 | 1 | 1 | 2.3 | 2.3 | ∞ |
| Test Sample Related | | | | | | | | | |
| Test Sample Positioning | E.4.2 | 3.12 | N | 1 | 1 | 1 | 3.1 | 3.1 | 35 |
| Device Holder Uncertainty | E.4.1 | 1.67 | N | 1 | 1 | 1 | 1.7 | 1.7 | 5 |
| Output Power Variation - SAR drift measurement | E.2.9 | 5 | R | 1.732 | 1 | 1 | 2.9 | 2.9 | ∞ |
| SAR Scaling | E.6.5 | 0 | R | 1.732 | 1 | 1 | 0.0 | 0.0 | ∞ |
| Phantom & Tissue Parameters | | | | | | | | | |
| Phantom Uncertainty (Shape & Thickness tolerances) | E.3.1 | 7.6 | R | 1.73 | 1.0 | 1.0 | 4.4 | 4.4 | ∞ |
| Liquid Conductivity - measurement uncertainty | E.3.3 | 4.3 | N | 1 | 0.78 | 0.71 | 3.3 | 3.0 | 76 |
| Liquid Permittivity - measurement uncertainty | E.3.3 | 4.2 | N | 1 | 0.23 | 0.26 | 1.0 | 1.1 | 75 |
| Liquid Conductivity - Temperature Uncertainty | E.3.4 | 3.4 | R | 1.732 | 0.78 | 0.71 | 1.5 | 1.4 | ∞ |
| Liquid Permittivity - Temperature Unceritainty | E.3.4 | 0.6 | R | 1.732 | 0.23 | 0.26 | 0.1 | 0.1 | ∞ |
| Liquid Conductivity - deviation from target values | E.3.2 | 5.0 | R | 1.73 | 0.64 | 0.43 | 1.8 | 1.2 | ∞ |
| Liquid Permittivity - deviation from target values | E.3.2 | 5.0 | R | 1.73 | 0.60 | 0.49 | 1.7 | 1.4 | ∞ |
| Combined Standard Uncertainty (k=1) | | | RSS | | | | 12.2 | 12.0 | 191 |
| Expanded Uncertainty (95% CONFIDENCE LEVEL) | | | k=2 | | | | 24.4 | 24.0 | |

The above measurement uncertainties are according to IEEE Std. 1528-2013